Chapter 3: The Classical Theory of Crystal Diffraction

Bragg

January 30, 2017

Contents

In the last two chapters, we learned that solids generally form periodic structures of different symmetries and bases. However, given a solid material, how do we learn what its periodic structure is? Typically, this is done by diffraction, where we project a beam (of either particles or radiation) at a solid with a wavelength $\lambda \approx$ the characteristic length scale of the lattice ($a \approx$ twice the atomic or molecular radii of the constituents). Diffraction of waves and particles (with de Broglie

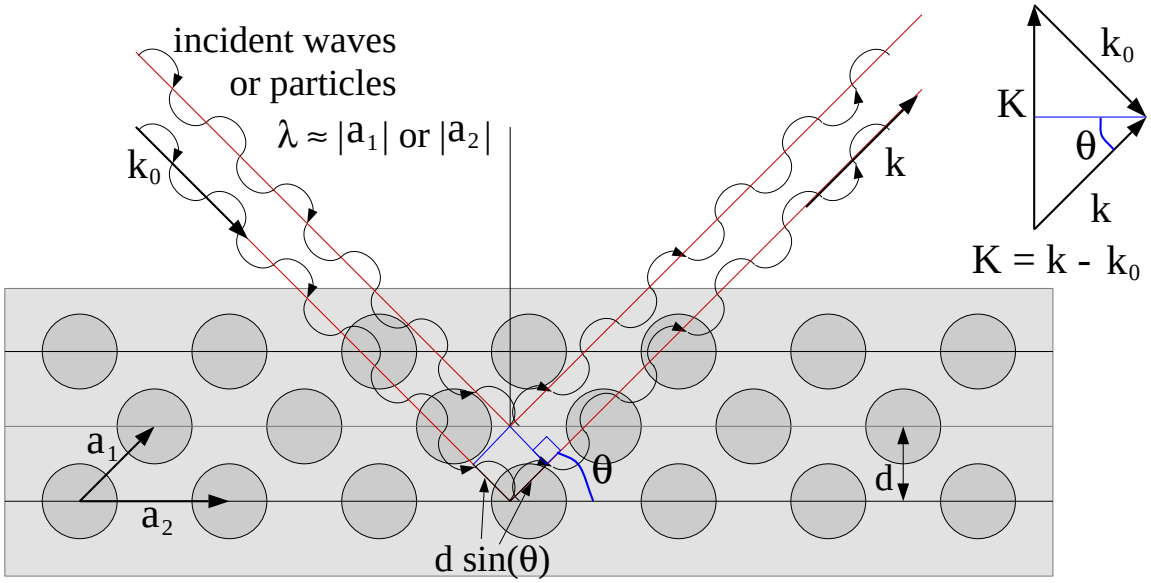

Figure 1: *Scattering of waves or particles with wavelength of roughly the same size as the lattice repeat distance allows us to learn about the lattice structure. Coherent addition of two particles or waves requires that* $2d\sin\theta = \lambda$ *(the Bragg condition), and yields a scattering maximum on a distant screen.*

wavelength $\lambda = h/p$) of $\lambda \approx a$ allows us to learn about the periodic structure of crystals. In a diffraction experiment one identifies Bragg peaks which originate from a coherent addition of scattering events in

multiple planes within the bulk of the solid.

However, not all particles with de Broglie wavelength $\lambda \approx a$ will work for this application. For example, most charged particles cannot probe the bulk properties of the crystal, since they lose energy to the scatterer very quickly. Recall, from classical electrodynamics, the rate at which particles of charge q, mass M, and velocity v lose energy to the electrons of charge e and mass m in the crystal is given roughly by

$$\frac{dE}{dx} \approx -\frac{4\pi n q^2 e^2}{m v^2} \ln\left(\frac{m\gamma^2 v^3}{qe\omega_0}\right) \sim \frac{q^2}{v^2}\,. \tag{1}$$

As an example, consider a non-relativistic electron scattering into a solid with $a \approx 2\mathbf{A}$. If we require that $a = \lambda = h/p = 12.3\times10^{-8}\mathrm{cm}/\sqrt{E}$ when E is measured in electron volts, then $E \approx 50\mathrm{eV}$. If we solve Eq. 1 for the distance δx where the initial energy of the incident is lost requiring that $\delta E = E$, when $n \approx 10^{23}/\mathrm{cm}^3$ we find that $\delta x \approx 100\mathbf{A}$. Thus, if $\lambda \approx a$, the electrons do not penetrate into the bulk of the sample (typically the first few hundred $\mathbf{A}$ of most materials are oxidized, or distorted by surface reconstruction of the dangling bonds at the surface, etc. See Fig. 2) Thus, electrons do not make a very good probe of the bulk properties of a crystal (instead in a process call low-energy electron diffraction, LEED, they may be used to study the surface of especially clean samples. I.e. to study things like surface reconstruction of the dangling bonds, etc.). Thus although they are obviously easier to accelerate (electrons or ion beams), they generally do not penetrate into the bulk and so tell us more about the surface properties of solids

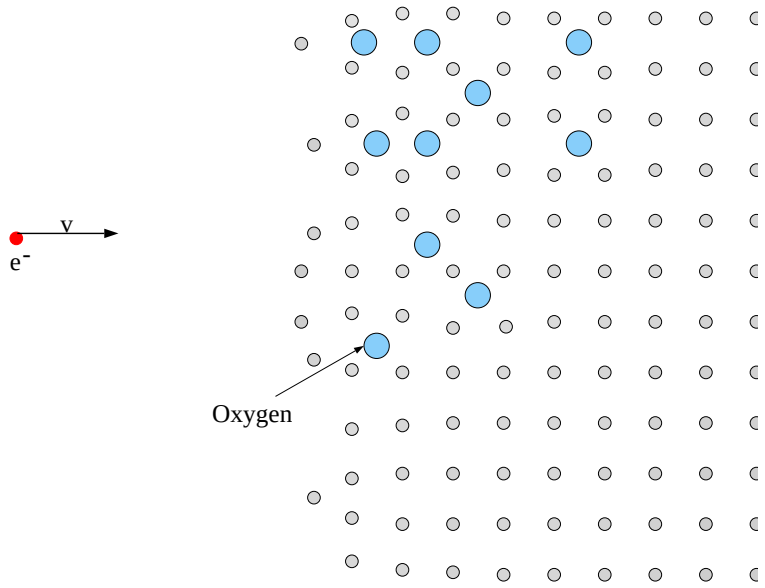

Figure 2: *An electron about to scatter from a typical material. However, at the surface of the material, oxidation and surface reconstruction distort the lattice. If the electron scatters from this region, we cannot learn about the structure of the bulk.*

which are often not representative of the bulk.

Thus the particle of the choice to determine bulk properties is the neutron which is charge neutral and scatters only from the nuclei. Radiation is often also used. Here the choice is only a matter of the wavelength used. X-rays are chosen since then $\lambda \approx a$

1 Classical Theory of diffraction

In this theory of diffraction we will be making three basic assumptions.

1. That the operator which describes the coupling of the target to the scattered "object" (in this case the operator is the density)

commutes with the Hamiltonian. Thus, this will be a classical theory.

2. We will assume some form of Huygens principle: that every radiated point of the target will serve as a secondary source spherical wavelets of the same frequency as the source and the amplitude of the diffracted wave is the sum of the wavelengths considering their amplitudes and relative phases. (For light, this is equivalent to assuming that it is unpolarized, and that the diffraction pattern varies quickly with scattering angle θ so that the angular dependence of a unpolarized dipole, $1 + (\cos\theta)^2$, may be neglected.)

3. We will assume that resulting spherical waves are not scattered again. In the fully quantum theory which we will derive later for neutron scattering, this will correspond to approximating the scattering rate by Fermi's golden rule (first-order Born approximation).

The basic setup of a scattering experiment is sketched in Fig. 3. Generally, we will also assume that $|R| \gg |r|$, so that we may always approximate the amplitude of the incident waves on the target as plane waves.

$$A_P = A_O e^{i(\mathbf{k}_0 \cdot (\mathbf{R}+\mathbf{r}) - \omega_0 t)} \,. \tag{2}$$

Then, consistent with the second assumption above,

$$A_B(R') \propto \int d^3 r A_P \rho(\mathbf{r}) \frac{e^{i\mathbf{k}\cdot(\mathbf{R}'-\mathbf{r})}}{|\mathbf{R}'-\mathbf{r}|} \,, \tag{3}$$

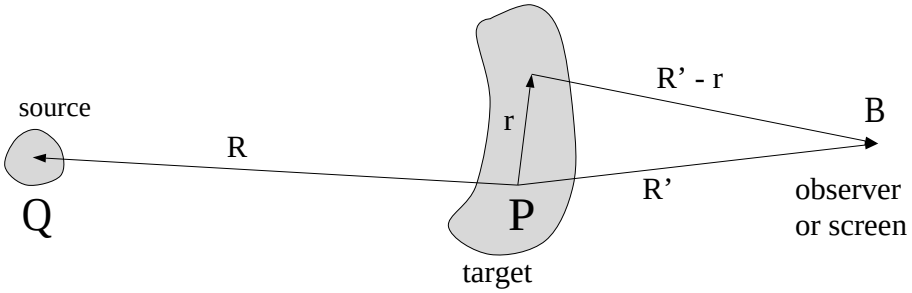

Figure 3: *Basic setup of a scattering experiment.*

which, after substitution of Eq.2, becomes

$$A_B(R') \propto A_O e^{i(\mathbf{k}_0\cdot\mathbf{R}+\mathbf{k}\cdot\mathbf{R}'-\omega_0 t)} \int d^3r \rho(\mathbf{r}) \frac{e^{-i(\mathbf{k}-\mathbf{k}_o)\cdot\mathbf{r}}}{|\mathbf{R}'-\mathbf{r}|} \,. \tag{4}$$

At very large R' (ie. in the radiation or far zone)

$$A_B(R') \propto \frac{A_O e^{i(\mathbf{k}_0\cdot\mathbf{R}+\mathbf{k}\cdot\mathbf{R}'-\omega_0 t)}}{R'} \int d^3r \rho(\mathbf{r}) e^{-i(\mathbf{k}-\mathbf{k}_o)\cdot\mathbf{r}} \,. \tag{5}$$

Or, in terms of the scattered intensity $I_B \propto |A_B|^2$

$$I_B \propto \frac{|A_O|^2}{R'^2} \left| \int d^3r \rho(\mathbf{r}) e^{-i(\mathbf{k}-\mathbf{k}_o)\cdot\mathbf{r}} \right|^2 \,. \tag{6}$$

The scattering intensity is just the absolute square of the Fourier transform of the density of scatterers. If we let $\mathbf{K} = \mathbf{k} - \mathbf{k}_0$ (cf. Fig. 1), then we get

$$I_B(\mathbf{K}) \propto \frac{|A_O|^2}{R'^2} \left| \int d^3r \rho(\mathbf{r}) e^{-i\mathbf{K}\cdot\mathbf{r}} \right|^2 = \frac{|A_O|^2}{R'^2} |\rho(\mathbf{K})|^2 \,. \tag{7}$$

From the associated Fourier uncertainty principle $\Delta k \Delta x \approx \pi$, we can see that the resolution of smaller structures requires larger values of $\mathbf{K}$ (some combination of large scattering angles and short wavelength of

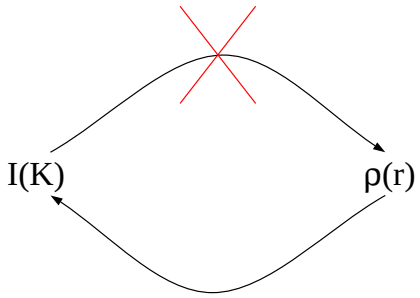

Figure 4: *Since the measured scattering intensity* $I(\mathbf{K}) \propto |\rho(\mathbf{K})|^2$ *the complex phase information is lost. Thus, a scattering experiment does not provide enough information to invert the transform* $\rho(\mathbf{r}) = \int \frac{d^3r}{(2\pi)^3} \rho(\mathbf{K}) e^{+i\mathbf{K}\cdot\mathbf{r}}$.

the incident light), consistent with the discussion at the beginning of this chapter.

In experiments the intensity I as a function of the scattering angle $\mathbf{K}$ is generally measured. In principle this is under-complete information. In order to invert the Fourier transform (which is a unitary transformation) we would need to know both the real and imaginary parts of

$$\rho(\mathbf{K}) = \int d^3r \rho(\mathbf{r}) e^{-i\mathbf{K}\cdot\mathbf{r}} \,. \tag{8}$$

Of course, if the experiment just measures $I \propto |\rho(\mathbf{K})|^2$, then we lose the relative phase information (i.e. $\rho(\mathbf{K}) = \rho_K e^{i\theta_K}$ so that $I \propto |\rho_K|^2$, and the phase information θ_K is lost). So, from a complete experiment, measuring $I(\mathbf{K})$ for all scattering angles, we do not have enough information to get a unique $\rho(\mathbf{r})$ by inverting the Fourier transform. Instead experimentalists analyze their data by proposing a feasible model structure (i.e. a $\rho(\mathbf{r})$ corresponding to some guess of which of one the 14 the

Bravais lattice and the basis), Fourier transform this, and compare it to the experimental data. The parameters of the model are then adjusted to obtain a best fit.

2 Scattering from Periodic Structures

Given this procedure, it is important to study the scattering pattern that would arise for various periodic structures. The density in a periodic crystal must have the same periodicity of the crystal

$$\rho(\mathbf{r}+\mathbf{r}_n)=\rho(\mathbf{r}) \quad \text{where} \quad \mathbf{r}_n = n_1\mathbf{a}_1 + n_2\mathbf{a}_2 + n_3\mathbf{a}_3 \tag{9}$$

for integer n_1, n_2, n_2. This also implies that the Fourier coefficients of ρ will be chosen from a discrete set. For example, consider a 1-d periodic structure

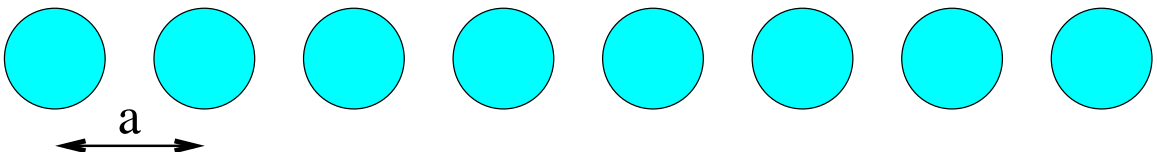

Figure 5:

$$\rho(x+na)=\rho(x)\,. \tag{10}$$

Then we must choose the G_n

$$\rho(x)=\sum_n \rho_n e^{iG_n x}\,, \tag{11}$$

so that

$$\begin{aligned}\rho(x+ma) &= \sum_n \rho_n e^{iG_n(x+ma)} = \sum_n \rho_n e^{iG_n(x)} e^{iG_n ma} \\ &= \sum_n \rho_n e^{iG_n(x)} = \rho(x)\,, \end{aligned} \tag{12}$$

I.e. $e^{iG_n ma} = 1$, or $G_n = 2n\pi/a$ where n is an integer.

This may be easily generalized to three dimensions, for which

$$\rho(\mathbf{r}) = \sum_{\mathbf{G}} \rho_{\mathbf{G}} e^{i\mathbf{G}\cdot\mathbf{r}} \tag{13}$$

where the condition of periodicity $\rho(\mathbf{r}+\mathbf{r}_n) = \rho(\mathbf{r})$ means that

$$\mathbf{G}\cdot\mathbf{r}_n = 2\pi m \quad m \in \mathcal{Z} \tag{14}$$

where $\mathcal{Z}$ is the group of integers (under addition). Now, lets consider $\mathbf{G}$ in some three-dimensional space and decompose it in terms of three independent basis vectors for which any two are not parallel and the set is not coplanar

$$\mathbf{G} = h\mathbf{g}_1 + k\mathbf{g}_2 + l\mathbf{g}_3\,. \tag{15}$$

The condition of periodicity then requires that

$$(h\mathbf{g}_1 + k\mathbf{g}_2 + l\mathbf{g}_3)\cdot n_1\mathbf{a}_1 = 2\pi m \quad m \in \mathcal{Z} \tag{16}$$

with similar conditions of the other principle lattice vectors $\mathbf{a}_2$ and $\mathbf{a}_3$. Since $\mathbf{g}_1$, $\mathbf{g}_2$ and $\mathbf{g}_3$ are not parallel or coplanar, the only way to satisfy this constraint for arbitrary n_1 is for

$$\mathbf{g}_1\cdot\mathbf{a}_1 = 2\pi \quad \mathbf{g}_2\cdot\mathbf{a}_1 = \mathbf{g}_3\cdot\mathbf{a}_1 = 0 \tag{17}$$

or some other permutation of 1 2 and 3, which would just amount to a renaming of $\mathbf{g}_1$, $\mathbf{g}_2$, and $\mathbf{g}_3$. The set ($\mathbf{g}_1$, $\mathbf{g}_2$, $\mathbf{g}_3$) are called the basis set for the reciprocal lattice. They may be constructed from

$$\mathbf{g}_1 = 2\pi \frac{\mathbf{a}_2 \times \mathbf{a}_3}{\mathbf{a}_1 \cdot (\mathbf{a}_2 \times \mathbf{a}_3)} \quad \text{plus cyclic permutations}\,. \tag{18}$$

It is easy to see that this construction satisfies Eq. 17, and that there is a one to one correspondence between the lattice and its reciprocal lattice. So, the reciprocal lattice belongs to the same point group as the real-space lattice[1].

2.1 The Scattering Intensity for a Crystal

Lets now apply this form for the density

$$\rho(\mathbf{r}) = \sum_{\mathbf{G}} \rho_{\mathbf{G}} e^{i\mathbf{G}\cdot\mathbf{r}} \tag{19}$$

to our formula for the scattering intensity

$$I_B(\mathbf{K}) \propto \frac{|A_O|^2}{R'^2} \left| \int d^3r \sum_{\mathbf{G}} \rho_{\mathbf{G}} e^{-i(\mathbf{K}-\mathbf{G})\cdot\mathbf{r}} \right|^2 \tag{20}$$

The integral above is simply

$$V\delta_{\mathbf{G},\mathbf{K}} = \begin{cases} V \text{ if } \mathbf{G} = \mathbf{K} \\ 0 \text{ if } \mathbf{G} \neq \mathbf{K} \end{cases}, \tag{21}$$

[1]One should note that this does not mean that the reciprocal lattice must have the same Bravais lattice structure as the real lattice. For example, the reciprocal of a fcc lattic is bcc and vice versa. This is consistent with the the statement that the reciprocal lattice belongs to the same point group as the real-space lattice since fcc and bcc share the O_h point group

where V is the lattice volume, so

$$I_B(\mathbf{K}) \propto \frac{|A_O|^2}{R'^2} |\rho_{\mathbf{G}}|^2 V^2 \delta_{\mathbf{G},\mathbf{K}} \tag{22}$$

This is called the Laue condition for scattering. The fact that this is proportional to V^2 rather than V just indicates that the diffractions spots, in this approximation, are infinitely bright (for a sample in the thermodynamic limit). Of course, this is because the spots are infinitely narrow or fine. When real broadening is taken into account, $I_B(\mathbf{K}) \propto V$ as expected.

Then as $G = h\mathbf{g}_1 + k\mathbf{g}_2 + l\mathbf{g}_3$, we can label the spots with the three integers $(h, k, l\ )$, or

$$I_{hkl} \propto |\rho_{hkl}|^2 \ . \tag{23}$$

Traditionally, negative integers are labled with an overbar, so $-h \to \overline{h}$. Then as $\rho(\mathbf{r})$ is real, $\rho_{\mathbf{G}} = \rho_{-\mathbf{G}}$, or

$$I_{\overline{hkl}} = I_{hkl} \quad \text{Friedel's rule} \tag{24}$$

Most scattering experiments are done with either a rotating crystal, or a powder made up of many crystalites. For these experiments, Friedel's rule has two main consequences

- For every spot at $\mathbf{k} - \mathbf{k}_0 = \mathbf{G}$, there will be one at $\mathbf{k}' - \mathbf{k}_0 = -\mathbf{G}$. Thus, for example if we scatter from a crystal with a 3-fold symmetry axis, we will get a six-fold scattering pattern. Clearly this can only happen, satisfy the Laue condition, and have $|\mathbf{k}| =$

$|\mathbf{k}_0|$, if the crystal is rotated by π in some axis perpendicular to the three-fold axis. In fact, single-crystal experiments are usually done either by mounting the crystal on a precession stage (essentially like an automotive universal joint, with the drive shaft held fixed, and the joint rotated over all angles), or by holding the crystal fixed and moving the source and diffraction screen around the crystal.

- The scattering pattern always has an inversion center, $\mathbf{G} \to -\mathbf{G}$ even when none is present in the target!

2.2 Bragg and Laue Conditions (Miller Indices)

Above, we derived the Laue condition for scattering; however, we began this chapter by reviewing the Bragg condition for scattering from adjacent planes. In this subsection we will show that, as expected, these are the some condition.

Consider the real-space lattice shown in Fig. 6. Highlighted by the solid lines are the parallel planes formed by $(1, 2, 2)$ translations along the principle lattice vectors $(\mathbf{a}_1, \mathbf{a}_2, \mathbf{a}_3)$, respectively. Typically these integers are labeled by (m, n, o), however, the plane is not typically labeled as the (m, n, o) plane. Rather it is labeled with the inverses

$$h' = 1/m \quad k' = 1/n \quad l' = 1/o\,. \tag{25}$$

Since these typically are not integers, they are multiplied by p, the

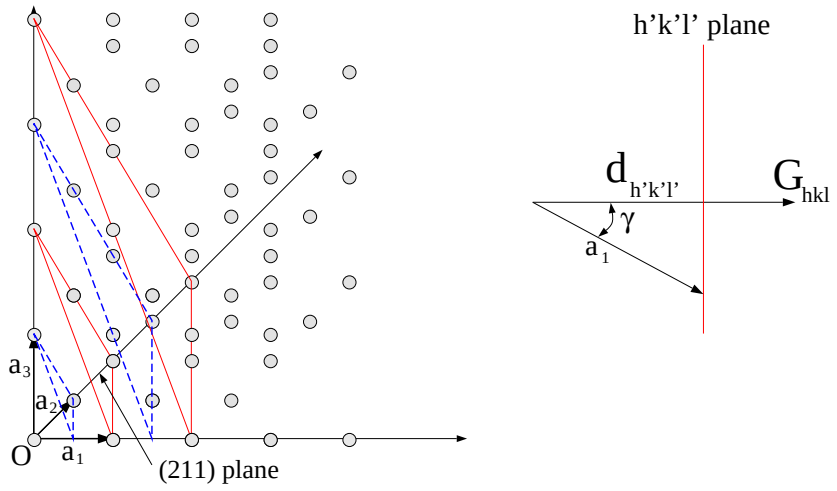

Figure 6: *Miller indices identification of planes in a lattice. Highlighted by the solid lines are the parallel planes formed by* $(1, 2, 2)$ *translations along the principle lattice vectors* $(\mathbf{a}_1, \mathbf{a}_2, \mathbf{a}_3)$*, respectively. Typically these integers are labeled by* (m, n, o)*, however, the plane is not typically labeled as the* (m, n, o) *plane. Rather it is labeled with the inverses* $h' = 1/m \quad k' = 1/n \quad l' = 1/o$*. Since these typically are not integers, they are multiplied by* p*, the smallest integer such that* $p(h', k', l') = (h, k, l) \in \mathcal{Z}$*. In this case,* $p = 2$*, and the plane is labeled as the* $(2, 1, 1)$ *plane. Note that the plane formed by* $(2, 4, 4)$ *translations along the principle lattice vectors is parallel to the* $(2, 1, 1)$ *plane.*

smallest integer such that

$$p(h', k', l') = (h, k, l) \in \mathcal{Z}\,. \tag{26}$$

In this case, $p = 2$, and the plane is labeled as the $(2, 1, 1)$ plane.

On may show that the reciprocal lattice vector $\mathbf{G}_{hkl}$ lies perpendicular to the (h, k, l) plane, and that the length between adjacent parallel planes $d_{hkl} = 2\pi/G_{hkl}$. To show this, note that the plane may be defined

by two non-parallel vectors $\mathbf{v}_1$ and $\mathbf{v}_2$ within the plane. Let

$$\mathbf{v}_1 = m\mathbf{a}_1 - n\mathbf{a}_2 = \mathbf{a}_1/h' - \mathbf{a}_2/k' \quad \mathbf{v}_2 = o\mathbf{a}_3 - n\mathbf{a}_2 = \mathbf{a}_3/l' - \mathbf{a}_2/k' \,. \tag{27}$$

Clearly the cross product, $\mathbf{v}_1 \times \mathbf{v}_2$ is perpendicular to the (h, k, l) plane

$$\mathbf{v}_1 \times \mathbf{v}_2 = -\frac{\mathbf{a}_3 \times \mathbf{a}_1}{h'l'} - \frac{\mathbf{a}_1 \times \mathbf{a}_2}{h'k'} - \frac{\mathbf{a}_2 \times \mathbf{a}_3}{k'l'} \,. \tag{28}$$

If we multiply this by $-2\pi h'k'l'/\mathbf{a}_1 \cdot (\mathbf{a}_2 \times \mathbf{a}_3)$, we get

$$\begin{aligned} &\frac{-2\pi h'k'l'\mathbf{v}_1 \times \mathbf{v}_2}{\mathbf{a}_1 \cdot (\mathbf{a}_2 \times \mathbf{a}_3)} = \\ &\frac{2\pi p}{p}\left[k'\frac{\mathbf{a}_3 \times \mathbf{a}_1}{\mathbf{a}_1 \cdot (\mathbf{a}_2 \times \mathbf{a}_3)} + l'\frac{\mathbf{a}_1 \times \mathbf{a}_2}{\mathbf{a}_1 \cdot (\mathbf{a}_2 \times \mathbf{a}_3)} + h'\frac{\mathbf{a}_2 \times \mathbf{a}_3}{\mathbf{a}_1 \cdot (\mathbf{a}_2 \times \mathbf{a}_3)}\right] = \\ &\mathbf{G}_{hkl}/p \end{aligned} \tag{29}$$

Thus, $\mathbf{G}_{hkl} \perp$ to the (h, k, l) plane. Now, if γ is the angle between $\mathbf{a}_1$ and $\mathbf{G}_{hkl}$, then the distance $d_{h'k'l'}$ from the origin to the (h', k', l') plane is given by

$$d_{h'k'l'} = m|\mathbf{a}_1|\cos\gamma = \frac{|\mathbf{a}_1|\mathbf{a}_1 \cdot \mathbf{G}_{hkl}}{h'|\mathbf{a}_1||\mathbf{G}_{hkl}|} = \frac{2\pi h}{h'G_{hkl}} = \frac{2\pi p}{G_{hkl}} \tag{30}$$

Then, as there are p planes in this distance (cf. Fig. 6), the distance to the nearest one is

$$d_{hkl} = d_{h',k',l'}/p = 2\pi/G_{hkl} \tag{31}$$

With this information, we can reexamine the Laue scattering condition $\mathbf{K} = \mathbf{k} - \mathbf{k}_o = \mathbf{G}_{hkl}$, and show that it is equivalent to the more intuitive Bragg condition. Part of the Laue is condition is that $|\mathbf{K}| = K = |\mathbf{k} - \mathbf{k}_0| = G_{hkl}$, now

$$K = 2k_0 \sin\theta = \frac{4\pi}{\lambda}\sin\theta \quad \text{and} \quad G_{hkl} = 2\pi/d_{hkl} \tag{32}$$

thus, the Laue condition implies that

$$1/d_{hkl} = 2\sin\theta/\lambda \quad \text{or} \quad \lambda = 2d_{hkl}\sin\theta \tag{33}$$

which is the Bragg condition. Note that the Laue condition is more

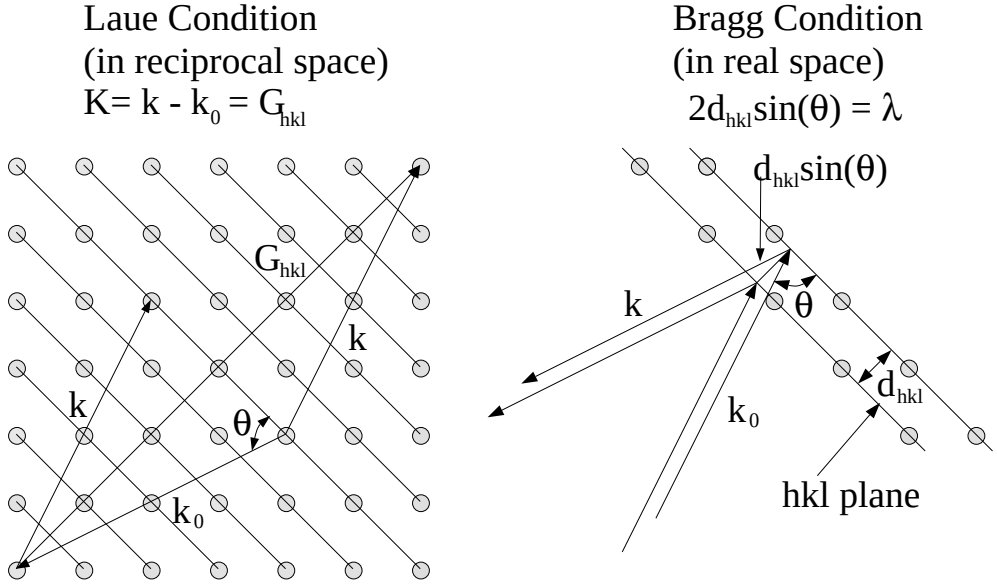

Figure 7: *Comparison of the Bragg* $\lambda = 2d_{hkl}\sin\theta$ *and Laue* $\mathbf{G}_{hkl} = \mathbf{K}_{hkl}$ *conditions for scattering.*

restrictive than the Bragg condition; it requires that *both* the magnitude and the direction of $\mathbf{G}$ and $\mathbf{K}$ be the same. However, there is no inconsistency here, since whenever we apply the Bragg condition, we assume that the plane defined by $\mathbf{k}$ and $\mathbf{k}_0$ is perpendicular to the scattering planes (cf. Fig. 7).

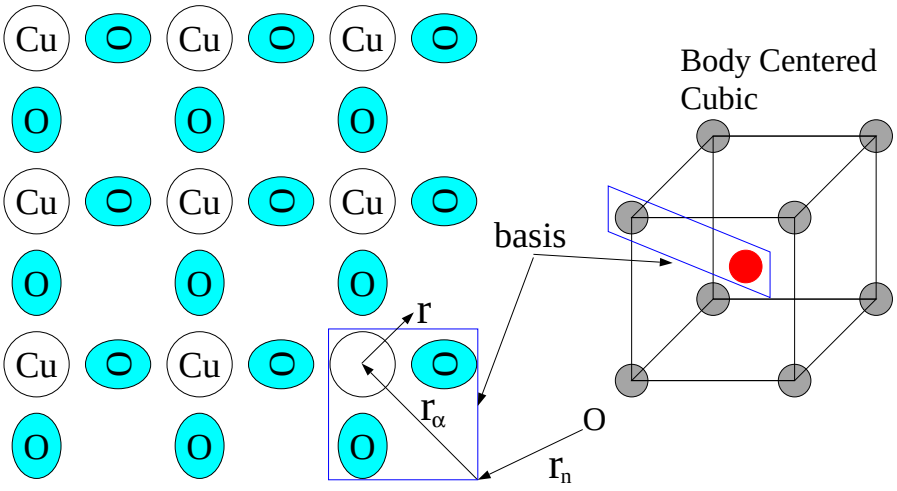

Figure 8: *Examples of lattices with non-trivial bases. The CuO_2 lattice (left) is characteristic of the cuprate high-temperature superconductors. It has a basis composed of one Cu and two O atoms imposed on a simple cubic lattice. The BCC lattice(right) can be considered as a cubic lattice with a basis including an atom at the corner and one at the center of the cube.*

2.3 The Structure Factor

Thus far, we have concentrated on the diffraction pattern for a periodic lattice ignoring the fine structure of the molecular of the basis. Examples of non-trivial molecular bases are shown in Fig. 8. Clearly the basis structure will effect the scattering (Fig. 9). For example, there will be interference from the scattering off of the Cu and two O in each cell. In fact, even in the simplest case of a single-element basis composed of a spherical atom of finite extent, scattering from one side of the atom will interfere with that from the other. In each case, the structure of the basis will change the scattering pattern due to interference of the waves scattering from different elements of the basis. The structure factors

account for these interference effects. The information about this interference, and the basis structure is contained in the atomic scattering factor f and the structure factor S.

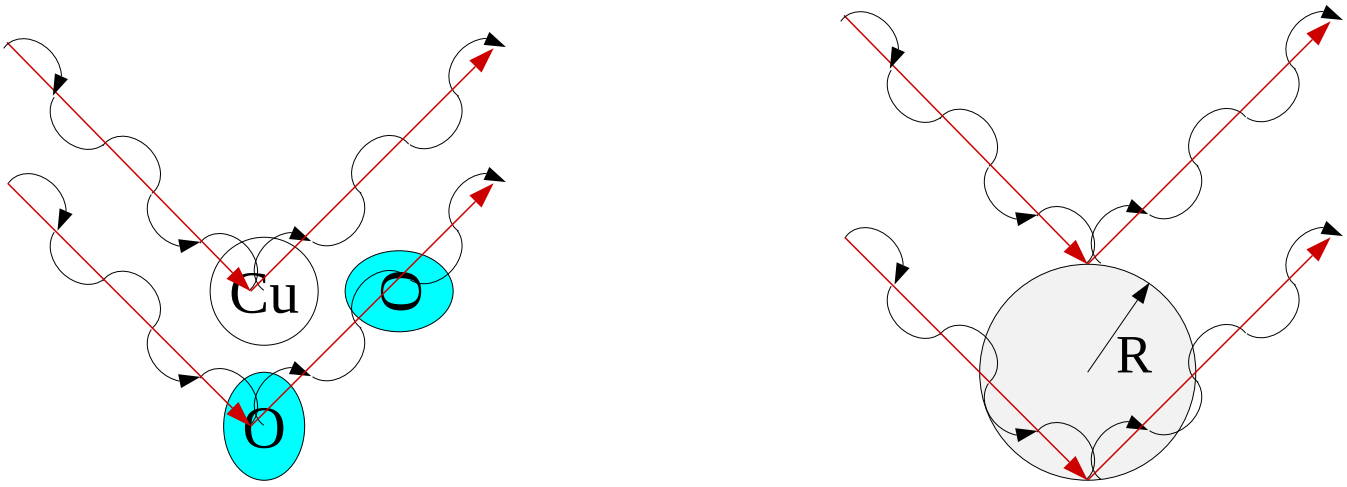

Figure 9: *Rays scattered from different elements of the basis, and from different places on the atom, interfere giving the scattered intensity additional structure described by the form factor S and the atomic form factor f, respectively.*

To show this reconsider the scattering formula

$$I_{hkl} \propto |\rho_{hkl}|^2 \tag{34}$$

The Fourier transform of the density may be decomposed into an integral over the basis cell, and a sum over all such cells

$$\begin{aligned} \rho_{hkl} &= \frac{1}{V}\int d^3r \rho(\mathbf{r}) e^{-i\mathbf{G}_{hkl}\cdot\mathbf{r}} = \frac{1}{V}\sum_{\text{cells}}\int_{\text{cell}} d^3r \rho(\mathbf{r}) e^{-i\mathbf{G}_{hkl}\cdot\mathbf{r}} \\ &= \frac{1}{V}\sum_{n_1,n_2,n_3}\int_{\text{cell}} d^3r \rho(\mathbf{r}) e^{-i\mathbf{G}_{hkl}\cdot(\mathbf{r}+\mathbf{r}_n)} \end{aligned} \tag{35}$$

where the location of each cell is given by $\mathbf{r}_n = n_1\mathbf{a}_1 + n_2\mathbf{a}_2 + a_3\mathbf{a}_3$.

Then since $\mathbf{G}_{hkl} \cdot \mathbf{r}_n = 2\pi m$, $m \in \mathcal{Z}$,

$$\rho_{hkl} = \frac{N}{V} \int_{\text{cell}} d^3 r \rho(\mathbf{r}) e^{-i\mathbf{G}_{hkl}\cdot\mathbf{r}} \tag{36}$$

where N is the number of cells and $\frac{N}{V} = 1/V_c$, V_c the volume of a cell. This integral may be further subdivided into an integral over the atomic density of each atom in the unit cell. If α labeles the different elements of the basis, each with density $\rho_\alpha(\mathbf{r}')$

$$\rho_{hkl} = \frac{1}{V_c} \sum_\alpha e^{-i\mathbf{G}_{hkl}\cdot\mathbf{r}_\alpha} \int d^3 r' \rho_\alpha(\mathbf{r}') e^{-i\mathbf{G}_{hkl}\cdot\mathbf{r}'} \tag{37}$$

The atomic scattering factor f and the structure factor may then be defined as parts of this integral

$$f_\alpha = \int d^3 r' \rho_\alpha(\mathbf{r}') e^{-i\mathbf{G}_{hkl}\cdot\mathbf{r}'} \tag{38}$$

so

$$\rho_{hkl} = \frac{1}{V_c} \sum_\alpha e^{-i\mathbf{G}_{hkl}\cdot\mathbf{r}_\alpha} f_\alpha = \frac{S_{hkl}}{V_c} \tag{39}$$

f_α describes the interference of spherical waves emanating from different points within the atom, and S_{hkl} is called the structure factor. Note that for lattices with an elemental basis $S = f$.

If we imagine the crystal to be made up of isolated atoms like that shown on the right in Fig. 9 (which is perhaps accurate for an ionic crystal) then, since the atomic charge density is spherically symmetric about the atom

$$\begin{aligned} f_\alpha &= \int d^3 r' \rho_\alpha(\mathbf{r}') e^{-i\mathbf{G}_{hkl}\cdot\mathbf{r}'} = -\int r'^2 dr' d(\cos\theta) d\phi \, \rho_\alpha(r') e^{-G_{hkl} r' \cos\theta} \\ &= 4\pi \int r'^2 dr' \rho(r') \frac{\sin G_{hkl} r'}{G_{hkl} r'} \,. \end{aligned} \tag{40}$$

As an example, consider a spherical atom of charge Ze^-, radius R, and charge density

$$\rho_\alpha(r') = \frac{3Z}{4\pi R^3}\theta(R - r') \tag{41}$$

then

$$\begin{aligned} f_\alpha &= \frac{3Z}{R^3}\int_0^R r'^2 dr' \frac{\sin G_{hkl} r'}{G_{hkl} r'} \\ &= -\frac{3Z}{(G_{hkl}R)^3}\left(\sin\left(G_{hkl}R\right) - \left(G_{hkl}R\right)\cos\left(G_{hkl}R\right)\right) \end{aligned} \tag{42}$$

This has zeroes whenever $\tan\left(G_{hkl}R\right) = G_{hkl}R$ and a maximum when $G_{hkl} = 0$, or in terms of the scattering angle $2k_0 \sin\theta = G_{hkl}$, when $\theta = 0, \pi$. In fact, we have that $f_\alpha(\theta = 0) = Z$. This is true in general, since

$$f_\alpha(\theta = 0) = f_\alpha(\mathbf{G}_{hkl} = 0) = \int d^3r' \rho_\alpha(\mathbf{r}') = Z\,. \tag{43}$$

Thus, for x-ray scattering $I \propto Z^2$. For this reason, it is often difficult to detect small-Z atoms with x-ray scattering.

2.3.1 The Structure Factor of Centered Lattices

Now let's look at the structure factor. An especially interesting situation occurs for centered lattices. We can consider a BCC lattice as a cubic unit cell $|\mathbf{a}_1| = |\mathbf{a}_2| = |\mathbf{a}_3|$, $\mathbf{a}_1 \perp \mathbf{a}_2 \perp \mathbf{a}_3$ and a two-atom basis $\mathbf{r}_\alpha = 0.5\alpha(\mathbf{a}_1 + \mathbf{a}_2 + \mathbf{a}_3)$, $\alpha = 0, 1$. Now if both sites in the unit cell ($\alpha = 0, 1$) contain the same atom with the same scattering factor f, then

$$\mathbf{r}_\alpha \cdot \mathbf{G}_{hkl} = 0.5\alpha(\mathbf{a}_1 + \mathbf{a}_2 + \mathbf{a}_3) \cdot (h\mathbf{g}_1 + k\mathbf{g}_2 + l\mathbf{g}_3) = \pi\alpha(h + k + l) \tag{44}$$

so that

$$\begin{aligned} S_{hkl} &= \sum_{\alpha=0,1} f e^{-i\pi\alpha(h+k+l)} \\ &= f(1+e^{-i\pi(h+k+l)}) = \begin{cases} 0 & \text{if } h+k+l \text{ is odd} \\ 2f & \text{if } h+k+l \text{ is even} \end{cases} \end{aligned} \tag{45}$$

This lattice gives rise to extinctions (lines, which appear in a cubic lattice, but which are missing here)! If both atoms of the basis are identical (like bcc iron), then the bcc structure leads to extinctions; however, consider CsCl. It does not have these extinctions since $f_{Cs^+} \neq f_{Cl^-}$. In fact, to a good approximation $f_{Cs^+} \approx f_{Xe}$ and $f_{Cl^-} \approx f_{Ar}$. However CsI (also a bcc structure) comes pretty close to having complete extinctions since both the Cs and I ions take on the Xe electronic shell. Thus, in the scattering pattern of CsI, the odd $h+k+l$ peaks are *much* smaller than the even ones. Other centered lattices also lead to extinctions.

In fact, this leads us to a rather general conclusion. The shape and dimensions of the unit cell determines the location of the Bragg peaks; however, the content of the unit cell helps determine the relative intensities of the peaks.

Extinctions in Binary Alloys Another, and significantly more interesting, example of extinctions in scattering experiments happens in binary alloys such as FeCo on a centered BCC lattice. Since Fe and Co are adjacent to each other on the periodic chart, and the x-ray form factor

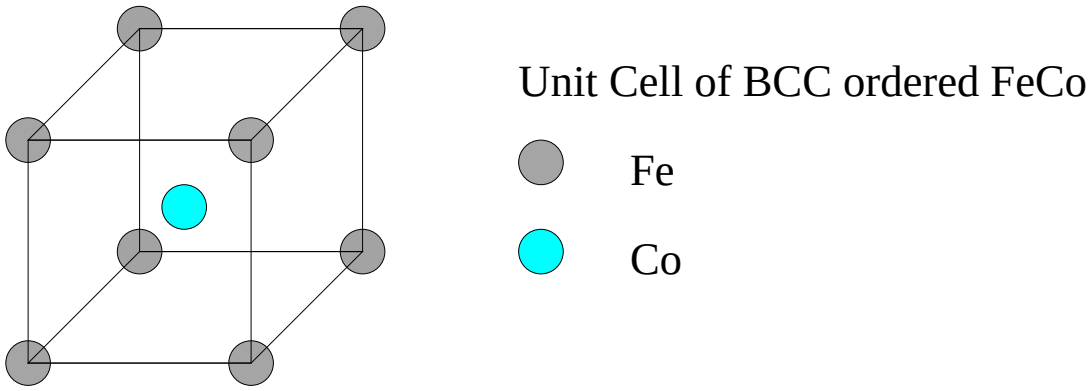

Figure 10: *The unit cell of body-centered cubic ordered FeCo.*

is proportional to Z ($Z_{\mathrm{Co}} = 27$, and $Z_{\mathrm{Fe}} = 26$)

$$f_{\mathrm{Fe}}^{\mathrm{x-ray}} \approx f_{\mathrm{Co}}^{\mathrm{x-ray}} \,. \tag{46}$$

However, since one has a closed nuclear shell and the other doesn't, their neutron scattering factors will be quite different

$$f_{\mathrm{Fe}}^{\mathrm{neutron}} \neq f_{\mathrm{Co}}^{\mathrm{neutron}} \tag{47}$$

Thus, neutron scattering from the ordered FeCo structure shown in Fig. 10 will not have extinctions; whereas scattering from a disordered structure (where the distribution of Fe and Co is random, so each site has a 50% chance of having Fe or Co, independent of the occupation of the neighboring sites) will have extinctions!

2.3.2 Powdered x-ray Diffraction

If you expose a columnated beam of x-rays to a crystal with a single crystalline domain, you usually will not achieve a diffraction spot. The

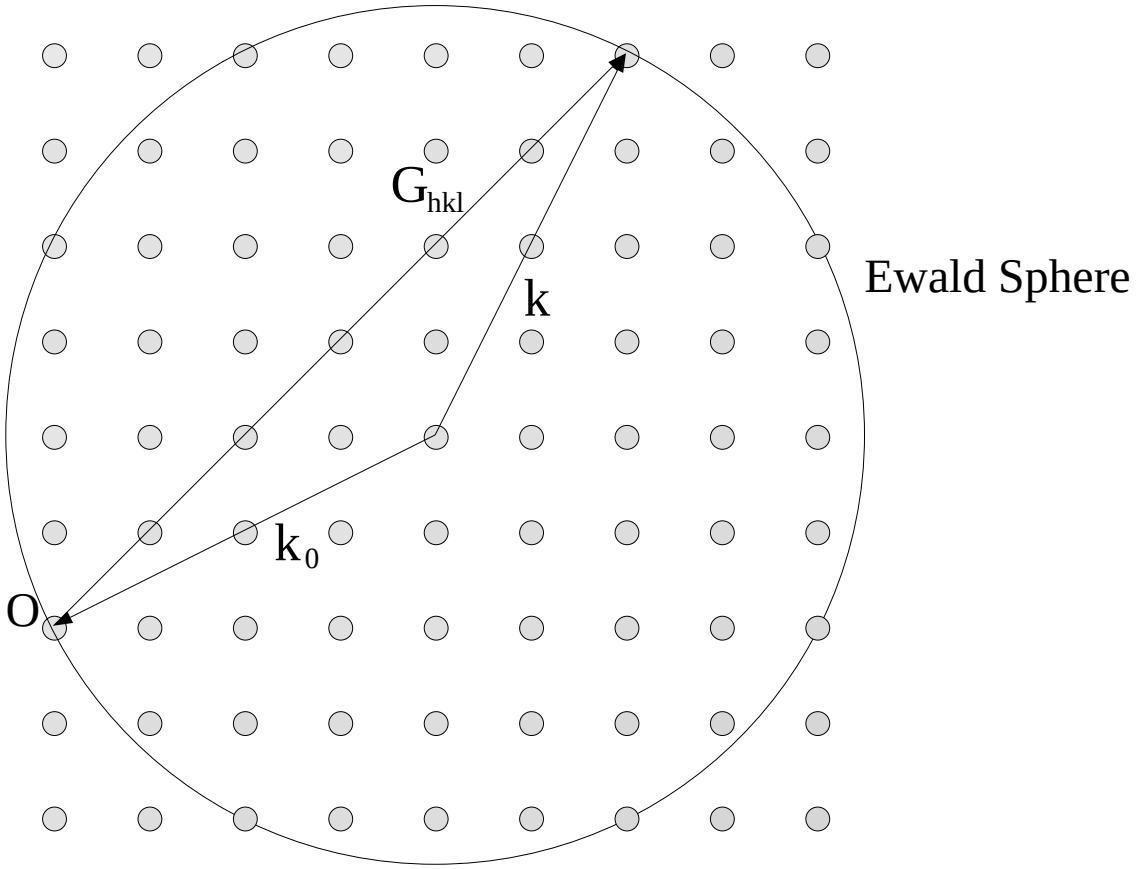

Figure 11: *The Ewald Construction to determine if the conditions are correct for obtaining a Bragg peak: Select a point in k-space as the origin. Draw the incident wave vector* $\mathbf{k}_0$ *to the origin. From the base of* $\mathbf{k}_0$*, spin* $\mathbf{k}$ *(remember, that for elastic scattering* $|\mathbf{k}| = |\mathbf{k}_0|$*) in all possible directions to form a sphere. At each point where this sphere intersects a lattice point in k-space, there will be a Bragg peak with* $\mathbf{G} = \mathbf{k} - \mathbf{k}_0$*. In the example above we find 8 Bragg peaks. If however, we change* $\mathbf{k}_0$ *by a small amount, then we have none!*

reason why can be seen from the Ewald construction, shown in Fig. 11 For any given $\mathbf{k}_0$, the chances of matching up so as to achieve $\mathbf{G} = \mathbf{k} - \mathbf{k}_0$ are remote. For this reason most people use powdered x-ray diffraction to characterize their samples. This is done by making a powder with randomly distributed crystallites. Exposing the powdered sample to x-rays and recording the pattern. The powdered sample corresponds to averaging over all orientations of the reciprocal lattice. Thus one will observe all peaks that lie within a radius of $2|\mathbf{k}_0|$ of the origin of the reciprocal lattice.